Modeling Phase Transition in Self-organized Mobile Robot Flocks*

Ali Emre Turgut, Cristián Huepe, Hande Çelikkanat, Fatih Gökçe, and Erol Şahin

KOVAN Res. Lab., Dept. of Computer Engineering
Middle East Technical University, Turkey
{aturgut,hande,fgokce,erol}@ceng.metu.edu.tr,
cristian@northwestern.edu

Abstract. We implement a self-organized flocking behavior in a group of mobile robots and analyze its transition from an aligned state to an unaligned state. We briefly describe the robot and the simulator platform together with the observed flocking dynamics. By experimenting with robotic and numerical systems, we find that an aligned-to-unaligned phase transition can be observed in both physical and simulated robots as the noise level is increased, and that this transition depends on the characteristics of the heading sensors. We extend the Vectorial Network Model to approximate the robot dynamics and show that it displays an equivalent phase transition. By computing analytically the critical noise value and numerically the steady state solutions of this model, we show that the model matches well the results obtained using detailed physics-based simulations.

1 Introduction

Flocks of birds, herds of quadrupeds and schools of fish stand as fascinating examples of self-organized coordination, where groups of individuals coherently move and maneuver in space as a collective unit [1,2]. Although it has long been studied in biology, it was Reynolds [3] who first demonstrated flocking in artificial systems, showing that realistic flocking behavior can be obtained in computer animation using a number of simple behaviors. Reynolds' seminal work generated interest in many different fields.

In robotics, Matarić [4] made one of the earliest attempts to obtain flocking in a group of robots by combining safe-wandering, aggregation, dispersion, and homing behaviors. She was able to demonstrate that a group of robots can "flock" towards a common homing direction while maintaining a cohesive grouping.

* The works of A.E. Turgut, F. Gökçe and E. Şahin are supported by TÜBİTAK under grant no: 104E066. The work of C. Huepe is supported by the National Science Foundation under Grant No. DMS-0507745. H.Çelikkanat acknowledges the partial support of the TÜBİTAK graduate student research grant. F. Gökçe is currently enrolled in Faculty Development Program (ÖYP) in Middle East Technical University on behalf of Süleyman Demirel University.

M. Dorigo et al. (Eds.): ANTS 2008, LNCS 5217, pp. 108–119, 2008.

In [5], Kelly and Keating used robots that can sense the obstacles as well as the relative range and bearing of their neighbors through a custom-made active infrared system. The robots used a radio-frequency system to elect one of them as the leader which would then wander in the environment while being followed by the others. In a recent study, Hayes et al. [6] proposed a "leaderless distributed flocking algorithm" consisting of two simpler behaviors: collision avoidance and velocity matching, using local center-of-mass calculations based on emulated range and bearing information. Additional studies in robotic flocking have been carried out in works such as [7,8].

Flocking has also attracted interest in physics, where various models have been proposed to study the emergence of *order* in such systems. The emergence of order corresponds to the collective self-alignment of the group to a common heading direction as a result of the interactions among its individuals. In a pioneering study, Vicsek et al. [9] proposed the Self-Driven Particles (SDP) model to explain the emergence of order in biological swarms. The SDP model uses massless and volumeless particles that move at a constant speed in a square arena with periodic boundary conditions. The heading of each particle is updated to the average direction of motion of its local neighbors and a noise term which is added to account for uncertainties in its inputs and control. Simulations of this model revealed that particles align if the system is above a critical mean density or if the magnitude of the noise is below a critical value. In a follow-up study, Gregoire et al. [10] extended the SDP model to add attraction and repulsion among the particles in their local neighborhood, thus achieving self-organized motion in an open domain.

Aldana et al. [11] proposed the Vectorial Network Model (VNM) to study the emergence of long-range order in systems with mostly local interactions. In the VNM, particles are placed in a two-dimensional lattice and their positions remain fixed. Each heading thus only determines here a pointing direction for a given lattice site. As in the SDP, headings are updated to the average pointing directions of its inputs, but here only some of these inputs are taken from neighboring lattice sites and the rest from randomly chosen (possibly distant) sites. The VNM simulations show that long-range order does not emerge at any nonzero noise value if the neighbors are chosen only locally. However, long-range order does emerge for sufficiently small noise values if a small fraction of the inputs are chosen from random particle sites. An interesting aspect of the VNM is that an analytic expression was obtained in [11] to describe its order-to-disorder phase transition for the case with no local interactions, where all inputs are taken from random particle sites.

Despite many efforts to control and model flocks in robotics and statistical physics, these two lines of research have remained relatively disconnected from each other. An exception can be found in the recent study in [12], where a link was established between the behavior of multi-robot systems and phase transitions. There have been two main reasons behind the failure to integrate both perspectives. First, until recently, true self-organized flocking behavior like the one observed in nature had not been achieved in robotic systems. Indeed,

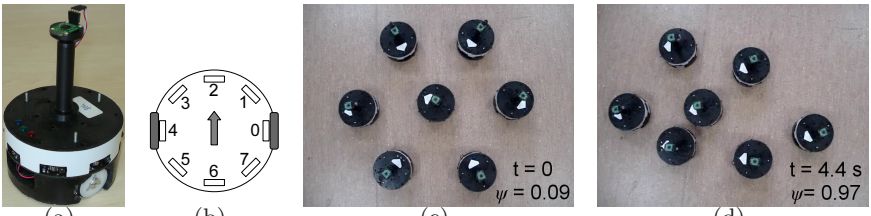

(a) (b) (c) (d)

Fig. 1. (a) Photo of a Kobot. (b) Top-view of a Kobot sketch showing the body (circle), the IR sensors (small numbered rectangles), and the two wheels (grey rectangles). (c-d) Starting from a disordered state, 7 Kobots negotiate a common heading and advance. White arrows on the robots indicate the forward direction.

the previous experimental studies in robotics used either a virtual or an explicit leader [5] to guide the group or assumed that a target heading (or destination) was sensed by the whole group [4,6,13]. Moreover, in some of these studies [6], the authors used "emulated sensors". Second, the assumptions required by the models developed in physics were often considered to be too unrealistic to be linked with studies conducted in robotics. The SDP model, for example, uses massless and volumeless mobile particles.

In [14], we reported the first true self-organized flocking on a group of mobile robots and showed that the robots can maneuver in an environment as a cohesive body while avoiding obstacles on their path. In this paper, we first demonstrate that the emergence of order in a robot flock depends on the amount of noise in the heading alignment behavior. We then extend the VNM to model the order-to-disorder phase transition that occurs in these robotic systems as the noise level is increased. Finally, we compare the predictions of the proposed model to the results obtained from robots.

2 Experimental Framework

We used a custom-built mobile robot platform, called Kobot, and its physics-based simulator, that we refer to as CoSS, in our experiments. Kobot is a CD-sized (with a 12 cm diameter), light-weight, differentially driven robotic platform (Figure 1(a)). It possesses an active Infrared Short-Range Sensing (IRSS) system designed for short-range proximity measurements. This system utilizes modulated infrared signals to minimize environmental interference and crosstalk among the robots. It consists of eight sensors placed evenly at 45° intervals (see Figure 1(b)), each of which is capable of sensing kin-robots and obstacles within a 21 cm range in seven discrete levels at 18 Hz.

The Virtual Heading Sensor (VHS) consists of a digital compass and a wireless communication module to receive the relative headings of neighboring robots. The VHS module measures its own heading with respect to the *sensed North* at each control step and broadcasts it to other robots through wireless communication. Each robot receives the broadcasted heading values within its

communication range. We define the set of robots that are "heard" by a given robot as its *VHS neighbors*. The angular difference between the broadcasted values and its own heading allows a robot to compute its relative heading with respect to its VHS neighbors and adjust it as needed. This operation of the VHS module assumes that the *sensed North* remains approximately the same among the robots within communication range.

Flocking Behavior. The flocking behavior [14] consists of a heading alignment and a proximal control combined in the weighted vector sum:

$$\boldsymbol{a} = \frac{1}{8}\boldsymbol{h} + \boldsymbol{p},$$

where $\boldsymbol{h}$ is the heading alignment vector, $\boldsymbol{p}$ is the proximal control vector, and $\boldsymbol{a}$ is the desired acceleration vector. The heading alignment vector $\boldsymbol{h}$, which is used to align the robot with the average heading of its neighbors, is calculated as:

$$\boldsymbol{h} = \frac{\sum_{j\in\mathcal{N}} e^{i\theta_j}}{\| \sum_{j\in\mathcal{N}} e^{i\theta_j} \|}$$

where $\mathcal{N}$ denotes the set of VHS neighbors, θ_j is the heading of the j^{th} neighbor and $\| \cdot \|$ calculates the Euclidean norm.

The proximal control behavior uses readings obtained from the IRSS to avoid collisions and to maintain cohesion between the robots. For each IR sensor, a virtual force proportional to the square of the difference between the measured distance and the desired distance is assumed. The desired distance (d_{des}) is defined as a finite value for other robots and ∞ for obstacles, in order to keep a fixed distance to its peers while moving away from obstacles. The normalized proximal control vector $\boldsymbol{p}$ is therefore given by:

$$\boldsymbol{p} = \frac{1}{8}\sum_k f_k e^{i\phi_k}$$

where $k \in \{0, 1, \cdots, 7\}$ denotes the sensor positioned at angle $\phi_k = \frac{\pi}{4}k$ with respect to the x-axis (see Figure 1(b)) and f_k is calculated as:

$$f_k = \begin{cases} -\frac{(d_k - d_{des})^2}{\frac{1}{8}} & \text{if } d_k \geq d_{des} \\ \frac{(d_k - d_{des})^2}{\frac{1}{8}} & \text{otherwise.} \end{cases}$$

The desired acceleration vector is mapped to the forward and angular velocities of the robot. The forward velocity u is modulated depending on the deviation of the desired acceleration vector from the current direction, as given by:

$$u = \begin{cases} 0.7\left(\frac{\boldsymbol{a}}{\|\boldsymbol{a}\|}.\hat{a}_c\right) & \text{if } \frac{\boldsymbol{a}}{\|\boldsymbol{a}\|}.\hat{a}_c \geq 0 \\ 0 & \text{otherwise} \end{cases}$$

where $\hat{a}_c$ is the current direction of the robot parallel to the y-axis of the body-fixed reference frame. The angular velocity ω is controlled by a proportional controller:

$$\omega = \frac{1}{2}(\angle\hat{a}_c - \angle\boldsymbol{a}).$$

The Order and Average Order Metrics. We evaluate the flocking performance by using the well-studied measure of order ψ [9], which corresponds to the average alignment of the group and is computed as:

$$\psi = \frac{1}{M} \left| \sum_{k=1}^{M} e^{i\theta_k} \right|,$$

where M is the number of robots and θ_k is the heading of the k^{th} robot. The order can take any value between 0 and 1. When individuals are aligned and the system is *ordered* we have $\psi \approx 1$, and when individuals are not aligned and the system is *disordered* we have $\psi \approx 0$. When the steady-state performance of the flocking behavior is considered, we will use the time average of the order, denoted by $\bar{\psi}$.

3 Modeling the Virtual Heading Sensor

The properties of the flocking behavior depend on two specific characteristics of the virtual heading sensor, namely: (1) the number of VHS neighbors that can be simultaneously detected, and (2) the nature and amount of noise in the digital compass measurements. Hence, we will study here the dependence of the system on these characteristics by modeling them with the CoSS simulator. The number of VHS neighbors N depends on the range of communication, the number of robots within this range, and the frequency and duration of this communication. Systematic analysis has shown that in the physical robots, the number of VHS neighbors can be as large as 20 in large groups.

The noise in VHS solely depends on the noise characteristics of the digital compass. In indoor environments, the presence of ferrous materials induce large amounts of noise on the digital compass. We model this noise by adding a vector of fixed magnitude in a random direction to each heading measurement [10,12]. The resulting noisy heading of the j^{th} neighbor received as input by a given

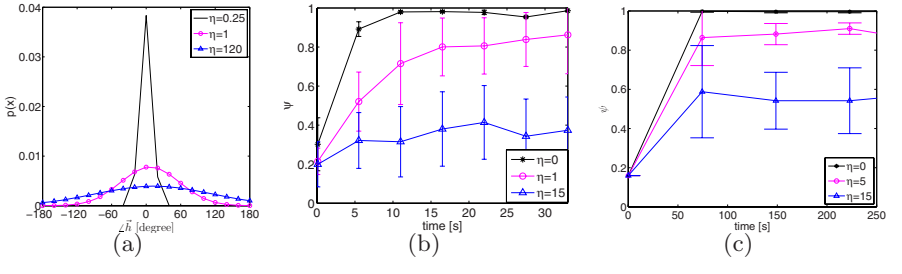

Fig. 2. (a) Probability density function of the simulated noisy measurement inputs of one VHS neighbor for different η values. (b) Evolution of ψ in time for 7 Kobots. (c) Evolution of ψ in time for 7 robots in the CoSS simulator. In this figure and subsequent figures the standard deviations are indicated using error bars.

robot is:

$$\theta_j = \angle(e^{i\theta_a} + \eta e^{i\xi})$$

where θ_a is the actual heading of the j^{th} neighbor, η is the magnitude of the noise vector, and $\angle(\cdot)$ is function that calculates the argument of a vector. The noise-vector direction ξ is a delta-correlated random variable with a uniform distribution in $[-\pi, \pi]$.

The probability density functions of the simulated noisy measurements is plotted in Figure 2(a) for various values of η. It is apparent that η determines the standard deviation of the resultant noisy headings, as expected.

4 Analysis of the Flocking Behavior

We investigate the effect of the sensing noise on the transient and on the steady-state to characterize the flocking phase transition in our system. The transient characteristics were investigated by conducting experiments with 7 Kobots and simulating 7 robots in CoSS for 1 VHS neighbor. The steady-state characteristics were investigated by simulating 100 robots in CoSS. The robots were initially placed in a regular hexagonal formation with a center-to-center distance of 25 cm having random orientations. Each experiment was repeated 10 times.

Transient Analysis. We varied the sensing noise on the VHS and measure the evolution of ψ in time for 7 Kobots in an actual experiment and for 7 robots in the CoSS simulator. In the Kobot experiments, the environmental noise is assumed to be negligible, so we set it to correspond to the $\eta = 0$ case. Higher η values are attained by adding noise artificially to each heading measurement. The evolution in time of ψ for the experimental and simulation cases are plotted on Figures 2(b) and 2(c). The results indicate that that ψ increases from a random initial condition, approaching approximately 1 when η is low, while settling to smaller ψ values when η is increased. Although the trends in the Kobot and CoSS cases are the same, Kobots perform worse than the robots in the CoSS simulation for the same amount of noise. This is probably due to the environmental noise in the Kobot experiments, that adds an unpredictable base noise level to the system.

Steady-State Analysis. We will now analyze the steady-state flocking behavior by finding the value of ψ at which the system settles for various noise levels. We consider the results of two sets of CoSS simulations: (1) runs with a small and a large number of robots (7 and 100, respectively), but with only 1 VHS neighbor, (2) runs with 100 robots and different numbers of VHS neighbors. Each simulation was conducted for 1000 s and its steady-state ψ value was calculated by averaging over the last 500 s. This guarantees that the steady-state condition has been achieved since it takes less than 250 s for ψ to converge. The results are plotted on Figures 3(a) and 3(b).

Figure 3(a) shows that, regardless of the flock size, an increase in η decreases the order. However, the order shows a much smaller decrease for the small group

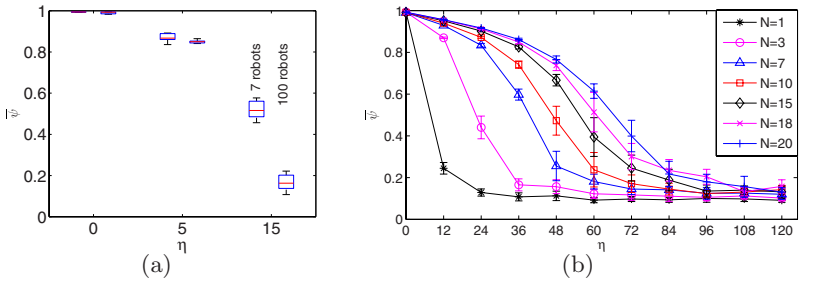

Fig. 3. (a) Plot of $\bar{\psi}$ measured in CoSS simulations containing 7 and 100 robots. The horizontal lines in the boxes, the box-ends, and the additional error bars correspond to the median and to its first and third quartiles, respectively. (b) Plot of $\bar{\psi}$ for 100 robots in CoSS for various N.

when $\eta = 15$. This is due to the finite size effects observed that are known to blur the difference between order and disordered collective states in small-sized statistical systems. In the rest, we will therefore focus on CoSS simulations with 100 robots, which enables reasonable run times while minimizing finite-size effects. It is apparent on Figure 3(b) that for all N values, ψ approaches 1 and the system organizes in a coherent flock as the noise level η is lowered to zero. If η is increased, ψ decreases and eventually approaches to 0. We also observe that increasing N increases the order of the flock for a constant η. The order-to-disorder transition that occurs by increasing the noise level in this robotic system is equivalent to the second-order phase-transition observed in various statistical physics systems. As in the physics context, we will refer to the η value at which the system loses all order as the critical noise level η_c.

5 Modeling the Phase Transition in Flocking

We are interested in modeling analytically the order-to-disorder phase transition observed in the flocking behavior of Kobots as a function of noise, and to determine η_c for a given number of VHS neighbors. We will consider a simple network-based model that includes the noise, interactions with randomly chosen agents, and an inertia-like term that captures qualitatively various local interactions that affect the Kobot dynamics. Our model does not, however, deal with all the complexities of the behavior. Indeed, in order to allow analytical solutions, it avoids any spatial description by representing agents as nodes interacting through random switching connections in a network. This model is an extension of the Vectorial Network Model (VNM) introduced in [11] as a network version of the SDP model in [9].

The original VNM can be solved analytically and is known to display an order-to-disorder transition similar to the one observed in Kobots, but it is not well adapted to describe some of the details of our robotic system. For example, the noise is introduced differently and the agents can turn in any direction at

every time-step, with no restrictions on the turning rate. We therefore introduce a new network system to model the Kobots, the Stiff-Vectorial Network Model (S-VNM), which we define as follows. At every time-step, each node updates its heading $h_j(t)$ based on N inputs chosen randomly from any node in the system, according to

$$\boldsymbol{h_j}(t+1) = \kappa e^{i\theta_j(t)} + \lambda \sum_{k=1}^{N} e^{i\theta_k(t)} + \eta \sum_{k=1}^{N} e^{i\xi_k(t)}. \tag{1}$$

Here, the heading h_j is a vector of arbitrary magnitude with $\angle[h_j] = \theta_j$, where the heading of Kobot j is given (in this network representation) by the angle θ_j associated to node j. The model parameters κ, λ, and η determine the relative importance of the persistence, interaction, and noise terms, respectively. The latter two correspond directly to the terms implemented in the VHS control part of the Kobot dynamics. Here, the noise is introduced as in [10], with a fixed magnitude η in a random direction given by ξ_k, a delta-correlated random variable uniformly distributed in $[-\pi, \pi]$. The persistence term models qualitatively an effective inertia that appears mainly due to the proximity interactions between Kobots. These make it harder for a given robot to turn in response to its VHS inputs or the noise since, if it is surrounded by other robots heading in the same direction, these will block it from shifting its heading.

Analytical Treatment of the S-VNM. One of the main appeals of the S-VNM lies in our ability to treat it analytically. We derive here a solution that allows us to compute the critical noise value η_c (at which the order-to-disorder transition occurs) in terms of κ, λ, and N. We will approach this problem as follows. First, we compute the probability density function (PDF) of each term in Equation (1). Then we impose that the PDF of θ_j (which is equal for all j) is the same at time t and at time $t+1$, which, together with Equation (1), provides us with a closed expression for the statistical steady state of this PDF. Finally, we find the value of η at which a constant distribution for θ_j becomes unstable. This corresponds to the critical noise level η_c above which there is a stationary distribution with h_j pointing in any direction with the same probability (the disordered state), and below which such solution is unstable, thus drifting the system to a distribution with a preferred direction for h_j (the ordered state). In what follows we will use the fact that the magnitude of h does not intervene in the dynamics of the S-VNM to rescale Equation (1) by dividing it by λ. We thus define $\tilde{\kappa} = \kappa/\lambda$ and $\tilde{\eta} = \eta/\lambda$ and use these rescaled variables below, dropping the tildes until the end of this calculation to simplify the notation.

We first consider the noise term, which can be viewed as the total displacement that results after taking N steps of length 1 in a two-dimensional random walk. Using this analogy, we can apply well-known random walk results and write the PDF of the position on the x y plane after N steps as

$$P_\eta(x, y) = \frac{1}{N\eta^2\pi} e^{-\frac{x^2+y^2}{N\eta^2}}. \tag{2}$$

We will need below the two-dimensional Fourier transform of Eq. 2, that can be readily computed to obtain

$$\hat{P}_\eta(\lambda_x, \lambda_y) = e^{-\frac{1}{4}N\eta^2(\lambda_x^2+\lambda_y^2)}. \tag{3}$$

We now carry out the calculation of the PDF of the interaction term, which can be quite involved. Fortunately, this result was already obtained in [11]. Assuming that all the θ_k have the same PDF and are statistically independent (which is true if the N inputs are all picked at random from any node in a large system), the Central Limit Theorem is used in [11] for large enough N values to find an approximate Gaussian expression for this PDF. Computing again its Fourier transform we obtain:

$$\hat{P}_{N\theta}(\lambda_x, \lambda_y) = e^{iN(\Delta_{1,0}\lambda_x+\Delta_{0,1}\lambda_y)-\frac{N}{2}(\sigma_c^2\lambda_x^2+\sigma_s^2\lambda_y^2+2\sigma_{cs}^2\lambda_x\lambda_y)} \tag{4}$$

where $\sigma_c^2(t) = \Delta_{2,0}(t) - [\Delta_{1,0}(t)]^2$, $\sigma_s^2(t) = \Delta_{0,2}(t) - [\Delta_{0,1}(t)]^2$, and $\sigma_{cs}^2(t) = \Delta_{1,1}(t) - \Delta_{1,0}\Delta_{0,1}$. Here, $\Delta_{m,n}(t)$ denotes the instantaneous cosine-sine moment of the angle distribution, given by

$$\Delta_{m,n}(t) = \int_{-\pi}^{\pi} P_\theta(\alpha; t)\cos^m(\alpha)\sin^n(\alpha)d\alpha,$$

in which $P_\theta(\alpha; t)$ is the PDF of the angle that describes the heading of each particle. Note that Eq. (4) converges very rapidly to the exact PDF of the interaction term as N is increased, providing a very good approximation for $N > 5$.

The derivations above furnish expressions for the PDF of every element of equation (1) in terms of the PDF of the direction of a single particle $P_\theta(\alpha; t)$. However, as they stand these expressions are far too complicated to find the functional form of $P_\theta(\alpha; t)$ as a stationary solution of Eq. (1). To continue the calculations, we will thus concentrate in solutions close to η_c. If $\eta > \eta_c$, the system is in the disordered regime and we know that all h_j must point in any direction with the same probability. This corresponds to having a uniform distribution $P_\theta(\alpha) = \frac{1}{2\pi}$. If $\eta < \eta_c$ we know that this PDF cannot be a stable stationary solution of the dynamics since the system becomes organized and the symmetry in the pointing directions of all h_j must be broken. Therefore, a small perturbation about the $P_\theta(\alpha)$ solution must grow in this regime. Without loss of generality, we can write a generic small perturbation of $P_\theta(\alpha)$ as:

$$P_\theta(\alpha) = \frac{1}{2\pi} + \delta\cos(\alpha), \tag{5}$$

where $\delta \ll 1$. Using this form for $P_\theta(\alpha; t)$, Eq. (4) becomes:

$$\hat{P}_{N\theta}(\lambda_x, \lambda_y) = e^{i\pi N\delta\lambda_x - \frac{1}{2}N\left[\left(\frac{1}{2}-\pi^2\delta^2\right)\lambda_x^2+\frac{\lambda_y^2}{2}\right]}. \tag{6}$$

We now can find the combined PDF of the interaction and noise terms by computing the inverse Fourier transform of the product of $\hat{P}_\eta(\lambda_x, \lambda_y)$ times $\hat{P}_{N\theta}(\lambda_x, \lambda_y)$ to obtain

$$P_{N\theta\eta}(x,y) = \frac{1}{\pi N\sqrt{(1+\eta^2)(1+\eta^2-2\pi^2\delta^2)}}\, e^{-\frac{1}{N}\left[\frac{(x-N\pi\delta)^2}{1+\eta^2-2\pi^2\delta^2}+\frac{y^2}{1+\eta^2}\right]}. \quad (7)$$

¿From this result we find the PDF of the Right Hand Side (RHS) of equation (1) by calculating the convolution of $P_{N\theta\eta}$ with $P_\theta(\alpha)$ (the PDF of the persistence term). The resulting expression is:

$$P_{RHS}(x,y) = \int_{-\pi}^{\pi} P_{N\theta\eta}(x-\kappa\cos\theta, y-\kappa\sin\theta)P_\theta(\theta)d\theta. \quad (8)$$

Expanding Eq. 8 to first order in the small δ perturbation, then expressing the resulting equation in polar coordinates (R,Φ) and integrating over R we finally obtain the PDF of the RHS

$$P_{RHS}(\Phi) = \frac{1}{2\pi} + \delta\Gamma\cos(\Phi), \quad (9)$$

where

$$\Gamma = \frac{\sqrt{\pi}\; e^{\frac{-\kappa^2}{2N(1+\eta^2)}}}{2\sqrt{N(1+\eta^2)}}\left[(N+\kappa)\, I_0\left(\frac{\kappa^2}{2N(1+\eta^2)}\right)+\kappa\, I_1\left(\frac{\kappa^2}{2N(1+\eta^2)}\right)\right]. \quad (10)$$

Here $I_n(\cdot)$ are the Modified Bessel Functions of the first kind, usually defined mathematically as the solutions to the differential equation: $z^2y'' + zy' - (z^2 + n^2)y = 0$.

In the stationary case, the LHS of Equation 1 is equal to $P_\theta(\phi)$. Hence, the LHS and the RHS have the same form and the condition for a statistically stationary solution $P_\theta(\Phi) = P_{RHS}(\Phi)$ becomes

$$\frac{1}{2\pi} + \delta\cos(\Phi) = \frac{1}{2\pi} + \lambda\Gamma\cos(\Phi). \quad (11)$$

The condition for $P_\theta(\alpha;t) = 1/(2\pi)$ to be a stable stationary solution of the probability distribution associated to the dynamics described in Eq. (1) is therefore given by $\Gamma < 1$. Setting Γ to 1, we thus find the critical noise level η_c at which the order-to-disorder transition occurs.

While $\Gamma = 1$ fully determines η_c implicitly in terms of the model parameters, this condition cannot be easily inverted to obtain an expression for η_c. We can find an explicit approximate form for η_c, however, by carrying out certain approximations in the regime that we are considering. We set κ and λ to 1.5 and 22, respectively, to capture the dynamics of the flocking behavior. For these coefficients, $\frac{\kappa^2}{2N(1+\eta^2)} \ll 1$, which makes $I_0() \sim 1$ and $I_1() \sim 0$. In the resulting expressions, the terms containing κ are small when compared to those containing other coefficients and, thus, they can be neglected. By then substituting $\eta = \tilde{\eta}\lambda$ we obtain the following simple approximate expression for η_c

$$\eta_c = \lambda\sqrt{\frac{N\pi}{4}}. \quad (12)$$

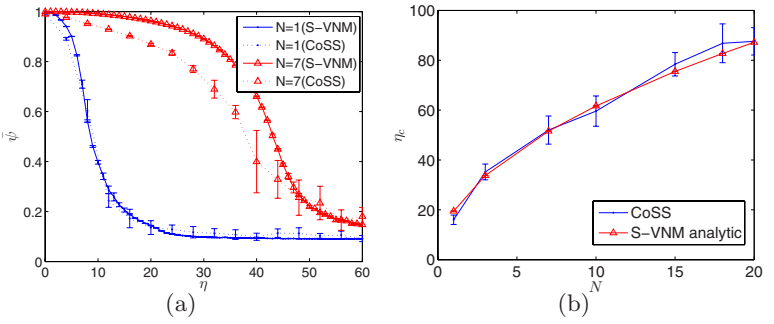

Fig. 4. (a) Phase transition diagram obtained numerically using S-VNM and CoSS simulations. (b) Critical noise values obtained using the analytical solution of S-VNM and CoSS simulations.

Results Using the S-VNM. The S-VNM can be utilized in two ways to predict the phase-transition in flocking. On one side, the S-VNM can be easily and efficiently implemented numerically to obtain the full phase-transition diagram for the stationary flocking solutions resulting from a given set of parameters. On the other side, we can use the analytical solution found above for the S-VNM to predict η_c as a function of N.

The steady-state response was investigated by simulating the S-VNM numerically. The simulations were performed with 100 particles for 10000 time-steps using $N = 1$ or $N = 7$. $\bar{\psi}$ for the last 5000 steps is plotted in Figure 4(a) as a function of η. On the same plot, $\bar{\psi}$ of analogous CoSS simulations is also displayed. It is apparent that predictions of the S-VNM are in close agreement with the CoSS results for $N = 1$. A slight deviation is observed in the $N = 7$ case as the system becomes organized.

Figure 4(b) displays the predicted critical noise value for the flocking behavior obtained using Eq. 12 together with results from CoSS simulations as a function of N. The two results are in close agreement both for small and large N values. However, we should note that Eq. 12 is actually only meant to be valid for relatively large values of N (typically at least $N > 5$) due to the use of the Central Limit Theorem in the analytical treatment.

6 Conclusion

In this paper we studied self-organized flocking in a group of mobile robots. We consider this work as a first step towards linking the mathematical models of flocking proposed in statistical physics with the results obtained in robotic systems. In this particular study, we showed the existence of an order-to-disorder phase transition in flocking and that the amount of noise as well as the number of neighbors with which each robot interacts determines the characteristics of this transition. We have extended the Vectorial Network Model to incorporate the dynamics of our robots and showed that the steady-state order characteristics

predicted by the model matches the ones obtained for the robotic system. This analysis shows that the proximal interactions among the robots can be crudely approximated by the inclusion of a stiffness term in the model.

References

1. Parrish, J.K., Viscido, S.V., Grünbaum, D.: Self-organized fish schools: An examination of emergent properties. Biol. Bull 202, 296–305 (2002)
2. Buhl, J., Sumpter, D.J.T., Couzin, I., Hale, J., Despland, E., Miller, E., Simpson, S.J.: From disorder to order in marching locusts. Science 312, 1402–1406 (2006)
3. Reynolds, C.: Flocks, herds and schools: A distributed behavioral model. In: Proc. of SIGGRAPH 1987, pp. 25–34 (1987)
4. Mataric, M.J.: Interaction and Intelligent Behavior. PhD thesis, MIT (1994)
5. Kelly, I., Keating, D.: Flocking by the fusion of sonar and active infrared sensors on physical autonomous robots. In: Proc. of the 3rd Int. Conf. on M2VIP, vol. 1, p. 14 (1996)
6. Hayes, A., Dormiani-Tabatabaei, P.: Self-organized flocking with agent failure: Offline optimization and demonstration with real robots. In: Proc. of ICRA 2002, pp. 3900–3905 (2002)
7. Fax, J.A., Murray, R.M.: Information flow and cooperative control of vehicle formations. IEEE Trans. Automat. Contr. 49(9), 1421–1603 (2004)
8. Sepulchre, R., Paley, D., Leonard, N.E.: Stabilization of planar collective motion: All-to-all communication. IEEE Trans. Automat. Contr. 52(5), 811–824 (2007)
9. Vicsek, T., Czirok, A., Ben-Jacob, E., Cohen, I., Shochet, O.: Novel type of phase transition in a system of self-driven particles. Physical Review Letters 75(6) (1995)
10. Gregoire, G., Chate, H., Tu, Y.: Moving and staying together without a leader. Physica D 181, 157–170 (2003)
11. Aldana, M., Huepe, C.: Phase transitions in self-driven many-particle systems and related non-equilibrium models: A network approach. J. of Stat. Phy. 112 (1/2), 135–153 (2003)
12. Baldassarre, G.: Self-organization as phase transition in decentralized groups of robots: A study based on boltzmann entropy. In: Mikhail, P. (ed.) Advances in Applied Self-Organizing Systems, pp. 127–146. Springer, Berlin (2008)
13. Campo, A., Nouyan, S., Birattari, M., Groß, R., Dorigo, M.: Negotiation of goal direction for cooperative transport. In: Dorigo, M., Gambardella, L.M., Birattari, M., Martinoli, A., Poli, R., Stützle, T. (eds.) ANTS 2006. LNCS, vol. 4150, pp. 191–202. Springer, Heidelberg (2006)
14. Turgut, A.E., Çelikkanat, H., Gökçe, F., Şahin, E.: Self-organized flocking with a mobile robot swarm. In: Proc. of AAMAS 2008, pp. 39–46 (2008)